Multiple Access Performance of Balanced UWB Transmitted-Reference Systems in Multipath

Tao Jia, *Student Member, IEEE*, and Dong In Kim, *Senior Member, IEEE*

***Abstract*— Recently, a novel balanced transmitted-reference (TR) system has been proposed for UWB communications. This TR system is capable of properly eliminating the inter-pulse interference (IPI) between the reference and data pulses in a single user multipath environment. In this paper, we investigate its multiple access (MA) performance by evaluating the second-order moments of noise and interference terms. The analytical framework developed here can also be used to accurately evaluate the MA performance of conventional TR system. It is shown that the proposed balanced TR system can achieve comparable MA capacity as conventional TR, while operating at higher information rate. On the other hand, given a target information rate, the balanced TR system in conjunction with M-ary signaling offers higher MA capacity than conventional TR system. The performance results suggest there exists a trade-off between the inter-pulse distance, thus the achievable information rate, and the MA capacity.**

***Index Terms*— Balanced TR system, inter-pulse interference (IPI), multiple access (MA) capacity, transmitted-reference (TR), ultra-wideband (UWB).**

I. Introduction

RECENTLY, there have been renewed interests on the transmitted-reference (TR) system for ultra-wideband (UWB) communications. The TR scheme, orignally proposed around 40 years ago [1], [2], was firstly applied to UWB communications by [3]. In a UWB-TR system, an unmodulated reference pulse is transmitted T_d seconds prior to each data-modulated pulse. The separation between the reference and data pulses is usually within the channel coherence time, in order for the two pulses to experience the same channel condition. On the other hand, this separation also needs to be larger than the channel delay spread, in order for the two pulses not to interfere with each other after passing through multipath channel. The TR receiver correlates the received signal with the one received T_d seconds earlier and integrates over a certain time interval to collect enough signal energy. In doing so, the reference pulse serves as the template and offers an immediate channel estimation for the detection of the data pulse, thus greatly reduces the complexity associated with channel estimation and timing synchronization in the commonly-used UWB Rake receiver.

However, in UWB-TR systems, the use of a noisy template results in noise-times-noise term, which is especially detrimental at low signal-to-noise ratio (SNR). To overcome this, there have been many proposals on improving the detection performance of UWB-TR systems. For example, in [4], the authors described and analyzed the performance of a receiver structure which averages multiple reference signals prior to the correlation, in order to obtain a cleaner template. In [5] and [6], the authors derived optimal/suboptimal TR receiver structures and showed that averaging multiple reference signals achieves a good trade-off between the system performance and complexity, considering the availability of symbol-long analog delay line, as stated in [16] and reference therein. In [7], the authors analyzed the performance of UWB-TR system based on the sampling expansion approach and investigated the validity of Gaussian approximation to noise statistics.

In the above works, the distance between the reference and data pulses is assumed to be at least equal to the channel delay spread such that there is no inter-pulse interference (IPI). This significantly limits the TR system's achievable information rate, since the channel delay spreads of UWB signals can be quite large [18]. If high data rates are targeted, this restriction may be released and the IPI has to be taken into account or dealt with effectively. In [8], the authors derived a discrete-time equivalent system model for differential TR system in the presence of inter-symbol interference (ISI). In [10], the authors proposed a maximum-likelihood template estimation for estimating the template for conventional TR system in the presence of IPI. However, the receiver complexity associated with maximum-likelihood estimation and storing multiple symbol waveforms can be prohibitively high. In [15], a dual pulse transmission scheme has been proposed to deal with the IPI. Alternatively, the authors in [11] proposed a balanced TR signaling scheme for UWB system, which is capable of fully eliminating the IPI by using a pair of matched-filters, thus offers increased information rate because the reference and date pulses can be separated at a distance much less than the channel delay spread.

On the other hand, there have been fewer research works on analyzing or improving the multiple access (MA) performance of UWB-TR systems under realistic multipath channel models. In [12], the authors analyzed the MA performance of both differential and conventional TR systems, by using the Q-function and evaluating the second-order moments of all noise and interference terms. Further, the validity of Gaussian

Manuscript received October 23, 2006; revised April 9, 2007 and October 4, 2007; accepted October 18, 2007. The associate editor coordinating the review of this paper and approving it for publication was D. Dardari. This work was supported by the MIC (Ministry of Information and Communication), Korea, under the ITRC (Information Technology Research Center) support program supervised by the IITA (Institute of Information Technology Assessment). This paper was presented in part at the IEEE GlobeCom'06 Conference, San Francsico, USA, Nov. 2006.

T. Jia is with the Bradley Department of Electrical and Computer Engineering, Virginia Tech, Blacksburg, VA 24061 USA (e-mail: taojia@vt.edu).

D. I. Kim is with the School of Information and Communication Engineering, Sungkyunkwan University, Suwon 440-746, Korea (e-mail: dikim@ece.skku.ac.kr).

Digital Object Identifier 10.1109/TWC.2008.060864.

approximation to the total inteference has been investigated. However, the analysis has not considered the effect of IPI. In addition, as our results suggest, the expression given by [eq. (21), 12] was somehow inaccurate. In [13], the authors proposed a scheme which assigns a pair of distinct user-specific signature sequences for both reference and data pulses and further evaluated the multiuser performance using the mean-based template estimator. In [14], a multi-pulse scheme was proposed for UWB-TR system and its performance in multiuser scenario has been evaluated.

In the above works on multiuser UWB-TR systems, less effort has been spent on investigating how a small inter-pulse distance (smaller than the channel delay spread) between the reference and data pulses will affect the TR system's MA capacity. On the other hand, an intuitive observation is that the IPI cancellation scheme proposed for a single-user UWB-TR system [11] may not work well due to the overwhelming multiple access interference (MAI) in a dense multiuser scenario. Therefore, an in-depth investigation into this issue can reveal how to achieve a trade-off between the system's achievable data rate and MA capacity. In this paper, we focus on our proposed signaling scheme which enables IPI cancellation and are more concerned with the receiver complexity issues. Specifically, we adopt a simple format of our proposed balanced TR system, whose receiver complexity is much reduced as compared to [11], and examine its performance in the presence of MAI, by evaluating the second-order moments of the noise and interference terms. We also demonstrate that the analysis developed here can also be used to evaluate the MA performance of conventional TR system. The performance results show that using the simple balanced TR receiver, we can achieve an MA capacity comparable to conventional TR while operating at higher information rate. Furthermore, if M-ary signaling is introduced, our proposed TR system can achieve higher MA capacity than conventional TR system, subject to the same information rate. Those performance results suggest that there exists a trade-off between the inter-pulse distance and the system's MA capacity, especially when the number of frames per symbol is large. Thus, depending upon the system's signal-to-noise ratio (SNR) and bit-error-rate (BER) requirements, we can trade the inter-pulse distance with the number of co-existing users that can be supported.

The rest of this paper is organized as follows. In Section II, we describe our proposed balanced TR system model. In Section III, we provide a detailed MA performance analysis, and also present an accurate MA performance analysis for conventional TR system. A brief description of M-ary orthogonal coded/balanced TR system with a suboptimal receiver is given in Section IV. Simulation and numerical results are presented in Section V. Concluding remarks are given in Section VI.

II. System Model

In balanced TR (BTR) system, the νth user's transmitted signal can be expressed as

$$s_{\text{tr}}^{(\nu)}(t) = \sum_{j=-\infty}^{+\infty} d_j^{(\nu)} \Big[w_{\text{tr}}(t - jT_f - c_j^{(\nu)} T_c) + b_{\lfloor j/N_s \rfloor}^{(\nu)} (-1)^j w_{\text{tr}}(t - jT_f - c_j^{(\nu)} T_c - T_d^{(\nu)}) \Big] \quad (1)$$

where $w_{\text{tr}}(t)$ is the unit-energy transmitted pulse of duration T_w. T_f is the frame time and N_s is the number of frames used to transmit one bit information. N_s is chosen to be an even number in order to enable the IPI cancellation mechanism, which will be explained later. In each frame, two pulses are transmitted. The first one is the reference pulse and the second, which is transmitted $T_d^{(\nu)}$ seconds later, is the data pulse. In our proposed TR system, $T_d^{(\nu)}$ does not have to be larger than the channel delay spread, denoted by T_{mds}, as opposed to conventional TR system. $c_j^{(\nu)}$ is the νth user's jth frame's TH code taking integer values, i.e., $c_j^{(\nu)} \in \{0, 1, \ldots, N_h^{(\nu)} - 1\}$, where $N_h^{(\nu)}$ is the νth user's maximum TH value. Note that, we have adopted a similar scheme as proposed in [12], for assigning user-specific values of $T_d^{(\nu)}$ and $N_h^{(\nu)}$, written as

$$T_d^{(\nu)} = T_d^{\min} + (\nu - 1)T_w, \quad N_h^{(\nu)} = N_h^{(N_u)} + (N_u - \nu) \quad (2)$$

where $\nu = 1, 2, \ldots, N_u$ and N_u is the total number of users. The primary purpose of assigning different $T_d^{(\nu)}$ to different users is to intentionally misalign an interferer's reference and data waveforms [12], so as to reduce the effect of MAI. The minimum inter-pulse distance $T_d^{\min}$ can be as small as one pulse duration T_w in the proposed BTR system. Also, note that $N_h^{(\nu)}$ has been set accordingly to maintain the same frame time T_f across all users. The frame time is set as $T_f = T_d^{(\nu)} + T_{\text{mds}} + N_h^{(\nu)} T_c$ with chip duration $T_c = T_w$, to avoid the inter-frame inteference (IFI) as well as the inter-symbol interference (ISI). The impact of IFI and ISI caused by a too small T_f has been investigated in [8] and is not the main concern of this paper. $\{d_j^{(\nu)}\}$ represents a user-specific pseudo-random sequence of values $\{-1, +1\}$ with equal probabilities to ensure a zero-mean signal output as well as to shape the transmit signal spectrum according to the FCC spectral mask. $b_i^{(\nu)}$ is the ith information bit of the νth user, where $b_i^{(\nu)} \in \{-1, +1\}$ with equal probabilities, and $\lfloor x \rfloor$ denotes the integer part of x. Note that in conventional TR (CTR) system, (1) and the definitions of all parameters remain same except that $T_d^{\min}$ is at least equal to T_{mds} and there will be no $(-1)^j$ weighting factor.

After transmitting through the channel, the received signal $r(t)$ corresponding to the ith bit of the *desired* first user can be written as $r(t) = s(t) + i(t) + n(t)$, where

$$s(t) = \sum_{j=iN_s}^{(i+1)N_s - 1} d_j^{(1)} \Big[g^{(1)}(t - jT_f - c_j^{(1)} T_c) + b_i^{(1)} (-1)^j g^{(1)}(t - jT_f - c_j^{(1)} T_c - T_d^{(1)}) \Big] \quad (3)$$

$$i(t) = \sum_{\nu=2}^{N_u} \sum_{j=-\infty}^{+\infty} d_j^{(\nu)} \Big[g^{(\nu)}(t - jT_f - c_j^{(\nu)} T_c - \tau^{(\nu)}) + b_{\lfloor j/N_s \rfloor}^{(\nu)} (-1)^j g^{(\nu)}(t - jT_f - c_j^{(\nu)} T_c - T_d^{(\nu)} - \tau^{(\nu)}) \Big] \quad (4)$$

represent the desired signal and the MAI, respectively. $g^{(\nu)}(t) = w_{\text{tr}}(t) \otimes h^{(\nu)}(t)$ ($\otimes$ denotes the convolution) is the received waveform corresponding to one transmitted pulse. $h^{(\nu)}(t)$ represents the channel impulse response of the νth user and is assumed to be invariant over at least one bit duration.

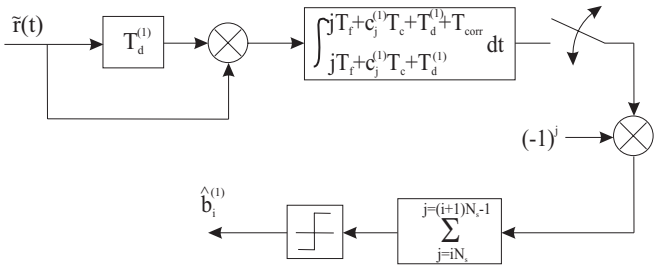

Fig. 1. Balanced TR receiver structure for the desired first user, that enables IPI cancellation in the digital domain.

$\tau^{(\nu)}$ is the νth user's asynchronous transmission delay relative to the first user where we have assumed $\tau^{(1)} = 0$ without loss of generality. $n(t)$ is the additive white Gaussian noise (AWGN) with two-sided power spectral density of $N_o/2$.

At the receiver, the received signal first passes through a front-end filter to suppress out-of-band noise. We assume an ideal low-pass filter with a cut-off frequency W has been used. This filtering output, denoted by $\tilde{r}(t)$ with an additional $\tilde{(\cdot)}$ indicating the filtering, is then fed to the receiver structure as shown in Fig. 1. As will be demonstrated in Section III, this receiver structure is capable of properly eliminating the IPI between the reference and data pulses occurred after passing through the multipath channel. Note that the receiver complexity has been considerably reduced compared to [11], in which the IPI cancellation is achieved by the pre-processing using additional matched-filters. Specifically, the matched-filter's impulse response is constructed based on the estimated received pulse waveform. In practice, different multipath components (MPCs) may experience different pulse distortions, which leads to the estimated pulse waveform less accurate. On the other hand, implementing the matched-filter's impulse response requires symbol-long analog delay line, which further increases the receiver complexity. However, the receiver structure shown in Fig. 1 achieves the IPI cancellation *via* the frame-rate correlation and does not require any pre-processing. Compared to CTR system, it only needs an additional weighting unit, which can easily be implemented in the digital domain.

To detect the first user's ith bit, the decision variable is compared to zero threshold, which produces $\hat{b}_i^{(1)} = \text{sign}\big(D_i\big)$. The decision variable D_i for the ith bit is given by

$$D_i = \sum_{j=iN_s}^{(i+1)N_s-1} (-1)^j\, D_{i,j} = \sum_{j=iN_s}^{(i+1)N_s-1} (-1)^j \times \int_{jT_f+c_j^{(1)}T_c+T_d^{(1)}}^{jT_f+c_j^{(1)}T_c+T_d^{(1)}+T_{\text{corr}}} \tilde{r}(t)\,\tilde{r}(t-T_d^{(1)})\,dt \qquad (5)$$

where the integration interval $0 < T_{\text{corr}} \le T_{\text{mds}}$ is chosen appropriately to collect enough signal energy as well as not to accumulate much noise energy. For notational simplicity, we define $\Omega_j^{(1)} \triangleq \Big[jT_f+c_j^{(1)}T_c+T_d^{(1)},\, jT_f+c_j^{(1)}T_c+T_d^{(1)}+T_{\text{corr}}\Big]$ to represent the integration range of (5).

III. Performance Analysis

Since the received signal is corrupted by the noise as well as the MAI, the jth frame's correlation output $D_{i,j}$ in (5) can be further written as

$$D_{i,j} = \xi_j + N_{1,j} + N_{2,j} + I_{1,j} + I_{2,j} + I_{3,j} \qquad (6)$$

where the six terms correspond to the desired signal, noise-times-signal, noise-times-noise, MAI-times-signal, MAI-times-noise and MAI-times-MAI, respectively. The decision variable D_i can thus be expressed in the same way as $D_i = \xi + N_1 + N_2 + I_1 + I_2 + I_3$.

It is easy to verify that N_1, N_2, I_1, I_2 and I_3 are zero-mean uncorrelated random variables.[1] Consequently, to investigate the bit-error rate (BER) performance of the proposed system in a semi-analytical way, we evaluate the desired signal as well as the second-order moments of the noise and interference terms one by one. After that, we use the Q-function to evaluate the BER conditioned on the channel realizations for all users and then average it over many channel realizations to finally obtain an unconditional BER. The validity of the implicit assumption that the composite of noise and interference terms has a Gaussian distribution is questionable, especially when the number of users is small. However, this is not the main focus of our paper and does not affect our idea.

A. Desired Signal Term ξ and IPI Cancellation

Based on (5) and (6), the desired signal is given by

$$\xi_j = \int_{\Omega_j^{(1)}} \tilde{s}(t)\,\tilde{s}(t-T_d^{(1)})\,dt. \qquad (7)$$

After substituting (3) into (7) and a few mathematical manipulations, (7) can be derived as

$$\begin{aligned}\xi_j = {} & (-1)^j\, b_i^{(1)} \int_0^{T_{\text{corr}}} \Big[\tilde{g}^{(1)}(t)\Big]^2\,dt \\ & + \int_{T_d^{(1)}}^{T_d^{(1)}+T_{\text{corr}}} \tilde{g}^{(1)}(t)\,\tilde{g}^{(1)}(t-T_d^{(1)})\,dt \\ & + \int_{T_d^{(1)}}^{T_d^{(1)}+T_{\text{corr}}} \tilde{g}^{(1)}(t-T_d^{(1)})\,\tilde{g}^{(1)}(t-2T_d^{(1)})\,dt \\ & + (-1)^j\, b_i^{(1)} \int_{T_d^{(1)}}^{T_d^{(1)}+T_{\text{corr}}} \tilde{g}^{(1)}(t)\,\tilde{g}^{(1)}(t-2T_d^{(1)})\,dt \end{aligned} \qquad (8)$$

where the second, third and fourth terms account for the IPI. The desired signal output is given by

$$\xi = \sum_{j=iN_s}^{(i+1)N_s-1} (-1)^j\,\xi_j \qquad (9)$$

which leads to

$$\begin{aligned}\xi = {} & b_i^{(1)} N_s \int_0^{T_{\text{corr}}} \Big[\tilde{g}^{(1)}(t)\Big]^2\,dt \\ & + b_i^{(1)} N_s \int_{T_d^{(1)}}^{T_d^{(1)}+T_{\text{corr}}} \tilde{g}^{(1)}(t)\,\tilde{g}^{(1)}(t-2T_d^{(1)})\,dt. \end{aligned} \qquad (10)$$

It is observed that, as long as N_s is an even number, the second and the third terms in (8) are fully cancelled out. Alternatively,

[1]Generally, due to the IPI occurred when the reference and data pulses are separated at a distance less than the channel delay spread T_{mds}, the MAI-times-MAI term I_3 is not zero mean. However, as will be verified later, our proposed BTR signaling scheme ensures it always has zero mean.

since those two terms are independent of the data, they can thus be regarded as bias terms, and then subtracted from the detection threshold as described in [9]. On the other hand, the fourth term in (8) can not be cancelled out and finally results in the second term in (10) which represents an additional fading term dependent on the channel condition, referred to as *residual* IPI. This residual IPI is, if not being estimated, generally not known to the receiver, thus will cause detection errors. By comparing this receiver with that of [11], we can find the receiver proposed in [11] achieves a complete IPI cancellation at the cost of increased receiver complexity, while the receiver here achieves a partial IPI cancellation, i.e., the presence of the residual IPI, due to the fact that the combining of the frame outputs occurs *after* the cross-correlation. However, this keeps the sampling rate as low as frame rate, which is one benefit of CTR system. In one word, we have implemented a low complexity receiver at the cost of some performance loss. It is worth noting that, as long as $T_d^{(1)} \geq T_{\text{mds}}/2$, the residual IPI becomes zero.

B. Noise Terms N_1 and N_2

After the front-end filtering using the ideal low-pass filter with cut-off frequency of W, the filtered noise $\tilde{n}(t)$ has an autocorrelation function $R_{\tilde{n}}(\tau) = N_o W \text{sinc}(2W\tau)$ where $\text{sinc}(x) \triangleq \sin(\pi x)/\pi x$. Again, based on (5) and (6), $N_{1,j}$ and $N_{2,j}$ are given by

$$N_{1,j} = \int_{\Omega_j^{(1)}} \Big[\tilde{s}(t)\tilde{n}(t - T_d^{(1)}) + \tilde{s}(t - T_d^{(1)})\tilde{n}(t)\Big] dt \quad (11)$$

$$N_{2,j} = \int_{\Omega_j^{(1)}} \tilde{n}(t)\tilde{n}(t - T_d^{(1)})\, dt. \quad (12)$$

After some necessary mathematical manipulations as shown in Appendix A, we can evaluate the second-order moments of N_1 and N_2, respectively, given by

$$\begin{aligned}\mathbf{E}\{{N_1}^2\} \cong \frac{N_s N_o}{2} \int_{T_d^{(1)}}^{T_d^{(1)}+T_{\text{corr}}} \Bigg\{ &\Big[\tilde{g}^{(1)}(t)\Big]^2 \\ &+ 2\Big[\tilde{g}^{(1)}(t - T_d^{(1)})\Big]^2 + \Big[\tilde{g}^{(1)}(t - 2T_d^{(1)})\Big]^2 \Bigg\} dt \\ &+ N_s N_o \int_{T_d^{(1)}}^{T_{\text{corr}}} \Big[\tilde{g}^{(1)}(t + T_d^{(1)})\, \tilde{g}^{(1)}(t - T_d^{(1)}) \\ &+ \tilde{g}^{(1)}(t)\, \tilde{g}^{(1)}(t - 2T_d^{(1)})\Big] dt \end{aligned} \quad (13)$$

$$\mathbf{E}\{{N_2}^2\} \cong \frac{1}{2} N_s {N_o}^2 W T_{\text{corr}}. \quad (14)$$

Note that in (13), the second integration results from the cross-correlation between the two integrands in (11) and if $T_d^{(1)} > T_{\text{corr}}$, it simply becomes zero. Furthermore, if $T_d^{(1)} > T_{\text{mds}}$, not only the second integration becomes zero, but also the first integration will only have its second integrand as non-zero, which finally yields the same result as in CTR system [12]. It is also to be noted that, in deriving (14), we have used the assumption that the time-bandwidth product WT_{corr} is large enough to validate the central limit theorem [7].

C. Interference Terms I_1, I_2 and I_3

In evaluating the second-order moments of the interference terms I_1, I_2 and I_3, we have made the following assumptions:

- other users' asynchronous transmission delays, namely $\tau^{(\nu)}$ for $\nu = 2, 3, \ldots, N_u$, are i.i.d. random variables and $\tau^{(\nu)}$ mod T_f is uniformly distributed over $[0, T_f)$;
- polarity codes $\{d_j^{(\nu)}\}$ are independent random variables and equiprobably take on $\{-1, +1\}$;
- data bits $\{b_i^{(\nu)}\}$ are independent random variables and equiprobably take on $\{-1, +1\}$.

First, the jth frame's MAI-times-signal term $I_{1,j}$ can be expressed as

$$I_{1,j} = \int_{\Omega_j^{(1)}} \Big[\tilde{s}(t)\,\tilde{i}(t - T_d^{(1)}) + \tilde{s}(t - T_d^{(1)})\,\tilde{i}(t)\Big] dt. \quad (15)$$

Based on (15), the second-order moment of I_1 can be evaluated in Appendix B.1 as

$$\begin{aligned}\mathbf{E}\{{I_1}^2\} = \frac{4N_s}{T_f} \sum_{\nu=2}^{N_u} \int_{-\infty}^{+\infty} \Big[&{R_{1\nu}}^2(\tau, 0) \\ &+ \frac{1}{2}\,{R_{1\nu}}^2(\tau - T_d^{(1)}, -T_d^{(1)}) + \frac{1}{2}\,{R_{1\nu}}^2(\tau, T_d^{(1)}) \\ &+ R_{1\nu}(\tau + T_d^{(1)}, T_d^{(1)})\, R_{1\nu}(\tau - T_d^{(1)}, 0) \\ &+ R_{1\nu}(\tau, 0)\, R_{1\nu}(\tau - T_d^{(1)}, -T_d^{(1)})\Big] d\tau \end{aligned} \quad (16)$$

where

$$R_{mn}(\tau, x) = \int_x^{x+T_{\text{corr}}} \tilde{g}^{(m)}(t)\, \tilde{g}^{(n)}(t - \tau)\, dt. \quad (17)$$

It is easy to find that if $x = T_d^{(1)} > T_{\text{mds}}$ or $x = -T_d^{(1)} < -T_{\text{mds}}$, (17) becomes zero regardless of τ. This means that, if $T_d^{(1)} > T_{\text{mds}}$, only the first term in (16) remains, which corresponds to the IPI-free case as in CTR system.

Next, we consider the second-order moment of the MAI-times-noise term I_2, whose contribution to the jth frame's desired signal can be written as

$$I_{2,j} = \int_{\Omega_j^{(1)}} \Big[\tilde{n}(t)\,\tilde{i}(t - T_d^{(1)}) + \tilde{n}(t - T_d^{(1)})\,\tilde{i}(t)\Big] dt. \quad (18)$$

Based on (18), we can evaluate the second-order moment of I_2 in Appendix B.1 as

$$\begin{aligned}\mathbf{E}\{{I_2}^2\} = \frac{2N_s N_o T_{\text{corr}}}{T_f} \sum_{\nu=2}^{N_u} \int_{-\infty}^{+\infty} \Bigg\{ &\Big[\tilde{g}^{(\nu)}(t)\Big]^2 + J_{\{T_{\text{corr}} > T_d^{(1)}\}} \\ &\times \frac{T_{\text{corr}} - T_d^{(1)}}{T_{\text{corr}}} \tilde{g}^{(\nu)}(t + T_d^{(1)}) \tilde{g}^{(\nu)}(t - T_d^{(1)}) \Bigg\} dt, \end{aligned} \quad (19)$$

where the indication $J_{\{T_{\text{corr}} > T_d^{(1)}\}}$ equals one if $T_{\text{corr}} > T_d^{(1)}$ and equals zero otherwise. Again, the second term in (19) results from the cross-correlation between the two integrands in (18).

Finally, we need to evaluate the second-order moment of the MAI-times-MAI term I_3, whose expression can be written as

$$I_3 = \sum_{j=iN_s}^{(i+1)N_s-1} (-1)^j I_{3,j} = \sum_{j=iN_s}^{(i+1)N_s-1} (-1)^j \int_{\Omega_j^{(1)}} \tilde{i}(t)\,\tilde{i}(t-T_d^{(1)})\,dt. \quad (20)$$

It is to be noted that I_3 can be further divided into two terms, depending upon whether it is caused by the correlation of the signals from the *same* user or *different* users. Specifically, if we write

$$\tilde{i}(t) = \sum_{\nu=2}^{N_u} \sum_{q=-\infty}^{+\infty} \tilde{i}_q^{(\nu)}(t)$$

where

$$\tilde{i}_q^{(\nu)}(t) \triangleq d_q^{(\nu)} \Big[\tilde{g}^{(\nu)}(t-qT_f-c_q^{(\nu)}T_c-\tau^{(\nu)}) + b_{\lfloor q/N_s \rfloor}^{(\nu)}(-1)^q \times \tilde{g}^{(\nu)}(t-qT_f-c_q^{(\nu)}T_c-T_d^{(\nu)}-\tau^{(\nu)})\Big], \quad (21)$$

the MAI-times-MAI term I_3 can be rewritten as the sum of two terms

$$I_3 = I_{3A}+I_{3B} = \sum_{j=iN_s}^{(i+1)N_s-1} (-1)^j I_{3A,j} + \sum_{j=iN_s}^{(i+1)N_s-1} (-1)^j I_{3B,j} \quad (22)$$

where the jth frame's contributions $I_{3A,j}$ and $I_{3B,j}$ are respectively given by

$$I_{3A,j} = \int_{\Omega_j^{(1)}} \sum_{\nu=2}^{N_u} \sum_{q,q'=-\infty}^{+\infty} \tilde{i}_q^{(\nu)}(t)\tilde{i}_{q'}^{(\nu)}(t-T_d^{(1)})dt \quad (23)$$

$$I_{3B,j} = \int_{\Omega_j^{(1)}} \sum_{\substack{\nu,\nu'=2,\\ \nu'\neq\nu}}^{N_u} \sum_{q,q'=-\infty}^{+\infty} \tilde{i}_q^{(\nu)}(t)\tilde{i}_{q'}^{(\nu')}(t-T_d^{(1)})dt. \quad (24)$$

Specifically, I_{3A} represents the total interference resulting from correlating the signals of the *same* interferer, referred to as self-MAI-times-MAI; while I_{3B} accounts for the total interference resulting from correlating the signals of *different* interferers, referred to as cross-MAI-times-MAI.

It is very easy to find that I_{3B} has zero mean, since different users' polarity codes and data bits in (21) are i.i.d. random variables taking on $\{\pm 1\}$ with equal probabilities, thus simply average to zero. On the other hand, in the presence of the IPI, I_{3A} is not necessarily zero-mean, especially in a CTR system. However, our BTR signaling scheme ensures that I_{3A} has a zero mean, as stated by the following lemma:

Lemma 1: Using the BTR signaling scheme, the self-MAI-times-MAI term I_{3A} has zero mean, namely

$$\mathbf{E}\{I_{3A}\} = 0.$$

Proof of lemma 1: see Appendix B.2.

It is also easy to verify that I_{3A} and I_{3B} are uncorrelated, again because of the independency among different users' polarity codes and data bits, which means $\mathbf{E}\{I_{3A}I_{3B}\} = 0$. The proof of this is omitted due to space limitations. Then, we simply have

$$\mathbf{E}\{{I_3}^2\} = \mathbf{E}\{{I_{3A}}^2\} + \mathbf{E}\{{I_{3B}}^2\}. \quad (25)$$

The second-order moments of I_{3B} and I_{3A} can then be evaluated in Appendixes B.3 and B.4, respectively, as

$$\mathbf{E}\{{I_{3B}}^2\} = \frac{4N_s}{{T_f}^2} \sum_{\substack{\nu,\nu'=2,\\ \nu'\neq\nu}}^{N_u} \int_0^{T_{\text{corr}}} \int_{-y}^{T_{\text{corr}}-y} C^{(\nu)}(x)C^{(\nu')}(x)dxdy \quad (26)$$

$$\mathbf{E}\{{I_{3A}}^2\} \cong \frac{N_s}{T_f} \sum_{\nu=2}^{N_u} \Bigg\{ \int_{-T_{\text{corr}}}^{T_{\text{mds}}} \Big[2R_{\nu\nu}^2(-T_d^{(1)},x) + R_{\nu\nu}^2(T_d^{(\nu)}+T_d^{(1)},x) + R_{\nu\nu}^2(T_d^{(\nu)}-T_d^{(1)},x)\Big]dx + \sum_{h\in\mathcal{H}^{(\nu)}} \frac{N_h^{(\nu)}-|h|}{{N_h^{(\nu)}}^2} \int_{-T_{\text{corr}}}^{T_{\text{mds}}} R_{\nu\nu}^2(T_f-T_d^{(1)}-T_d^{(\nu)}-hT_c,x)\,dx + \sum_{h_1\in\mathcal{H}^{(\nu)}} \sum_{h_2\in\mathcal{H}^{(1)}} \frac{N_h^{(\nu)}-|h_1|}{{N_h^{(\nu)}}^2} \times \frac{N_h^{(1)}-|h_2|}{{N_h^{(1)}}^2} \times \int_{-T_{\text{corr}}}^{T_{\text{mds}}} \Big[\frac{X_{N_s}}{N_s} R_{\nu\nu}(T_d^{(\nu)}-T_d^{(1)},x) \times R_{\nu\nu}(T_d^{(\nu)}-T_d^{(1)},x+h_1T_c+h_2T_c) + \frac{X_{N_s}}{N_s} \times R_{\nu\nu}(T_d^{(\nu)}+T_d^{(1)},x)R_{\nu\nu}(T_d^{(\nu)}+T_d^{(1)},x+h_1T_c+h_2T_c) - 2R_{\nu\nu}(-T_d^{(1)},x)\,R_{\nu\nu}(-T_d^{(1)},x+h_1T_c+h_2T_c)\Big]dx \Bigg\} \quad (27)$$

where

$$C^{(\nu)}(x) = \int_0^{T_{\text{mds}}} \tilde{g}^{(\nu)}(t)\,\tilde{g}^{(\nu)}(t-x)\,dt,$$

$$\mathcal{H}^{(\nu)} = \{k:\ k \text{ is integer}, \quad -N_h^{(\nu)}+1 \le k \le N_h^{(\nu)}-1\}$$

$$X_{N_s} = \frac{1}{3}(N_s-1)(2N_s-1)$$

For tractable and possible result, in deriving (27), several approximations have been made by ignoring some of the insignificant cross-terms. Finally, the bit-error rate (BER) conditioned on one channel realization can be evaluated by using the Q-function and substituting (10), (13), (14), (16), (19), (26) and (27) for calculating the signal-to-interference-plus-noise ratio (SINR).

D. Special Case: MA Performance for CTR System

As we mentioned earlier, the above analysis includes the MA performance for CTR system as a special case. Specifically, for CTR system, i.e., when $T_d^{\min} \ge T_{\text{mds}}$, our results of the desired signal ξ^{conv} and the second order moments of N_1^{conv}, N_2^{conv}, I_1^{conv}, I_2^{conv} are same as those derived in [12]. For I_{3B}^{conv}, there is a slight difference regarding the summation, shown below as $\nu' \neq \nu$,

$$\mathbf{E}\{{I_{3B}^{\text{conv}}}^2\} = \frac{4N_s}{{T_f}^2} \sum_{\substack{\nu,\nu'=2,\\ \nu'\neq\nu}}^{N_u} \int_0^{T_{\text{corr}}} \int_{-y}^{T_{\text{corr}}-y} C^{(\nu)}(x)C^{(\nu')}(x)\,dx\,dy. \quad (28)$$

In addition, for I_{3A}^{conv}, our result is

$$\mathbf{E}\{{I_{3A}^{\text{conv}}}^2\} \cong \frac{N_s}{T_f} \sum_{\nu=2}^{N_u} \Bigg\{ \int_{-T_{\text{corr}}}^{T_{\text{mds}}} R_{\nu\nu}^2(T_d^{(\nu)}-T_d^{(1)},x)\,dx \quad (29)$$

$$+\sum_{h\in\mathcal{H}^{(\nu)}}\frac{N_h^{(\nu)}-|h|}{{N_h^{(\nu)}}^2}\int_{-T_{\rm corr}}^{T_{\rm mds}}R_{\nu\nu}^2(T_f-T_d^{(1)}-T_d^{(\nu)}-hT_c,x)\,dx\Bigg\}$$

$$+\frac{X_{N_s}}{N_sT_f}\sum_{\nu=2}^{N_u}\sum_{h_1\in\mathcal{H}^{(\nu)}}\sum_{h_2\in\mathcal{H}^{(1)}}\frac{N_h^{(\nu)}-|h_1|}{{N_h^{(\nu)}}^2}\times\frac{N_h^{(1)}-|h_2|}{{N_h^{(1)}}^2}$$

$$\times\int_{-T_{\rm corr}}^{T_{\rm mds}}R_{\nu\nu}(T_d^{(\nu)}-T_d^{(1)},x)R_{\nu\nu}(T_d^{(\nu)}-T_d^{(1)},x+h_1T_c+h_2T_c)\,dx.$$

The derivation is provided in Appendix B.5, along with some simulation in the results section.

IV. M-ary Orthogonal Coded/Balanced TR System

Based on our BTR signaling scheme, we can easily incorporate an M-ary orthogonal modulation to increase the data rate. Specifically, the νth user's transmitted signal in M-ary orthogonal coded/balanced TR (MBTR) system is given by

$$s_{\rm tr}^{(\nu)}(t)=\sum_{j=-\infty}^{+\infty}d_j^{(\nu)}\Big[w_{\rm tr}(t-jT_f-c_j^{(\nu)}T_c)+b_{\lfloor j/N_s\rfloor}^{(\nu)}\times e_{{\rm mod}(j,N_s)}^{k^{(\nu)}}w_{\rm tr}(t-jT_f-c_j^{(\nu)}T_c-T_d^{(\nu)})\Big]. \quad (30)$$

Here, $e_n^{k^{(\nu)}}$ is the nth element of the $k^{(\nu)}$th orthogonal *balanced* sequence,[2] where $k^{(\nu)}\in\{0,1,\ldots,M-1\}$ with $M\le N_s-1$, is determined by the νth user's additional $\log_2 M$ information bits. Therefore, together with the original one bit carried by the polarity modulation, i.e., $b_{\lfloor j/N_s\rfloor}^{(\nu)}$, each *symbol* represents $(1+\log_2 M)$ bits. For the detection of the first user's ith symbol, the mth decision statistic is formulated as

$$\xi_{i,m}=\sum_{j=iN_s}^{(i+1)N_s-1}e_{{\rm mod}(j,N_s)}^{m}\int_{\Omega_j^{(1)}}\tilde{r}(t)\,\tilde{r}(t-T_d^{(1)})\,dt \quad (31)$$

for $m=0,1,\ldots,M-1$. Then, the $(1+\log_2 M)$ bits can be detected according to one of M decision statistics, whichever yields the maximum absolute value. Note that the receiver structure described here differs from the one proposed in [11], in the sense that this receiver does not require the matched-filter based pre-processing and thus has lower complexity at the cost of degraded performance. Since M-ary signaling effectively increases the information rate, the frame time can be increased subject to a fixed target information rate, thus allowing more space for TH.

V. Results

To first validate our analyses for BTR system, we have used IEEE 802.15.3a channel models for simulation purposes [18]. Without loss of generality, we will only present the results for CM1, which represents a line-of-sight (LOS) channel measurement with a transceiver separation of 0-4m. The continuous-time channel impulse response is sampled at 40 GHz, then convolved with the received pulse, finally downsampled to 6 GHz to generate the received waveform. The received pulse is assumed to be the second-order derivative of Gaussian pulse with pulse width of 0.7ns (equal to the chip time T_c). The channel delay spread $T_{\rm mds}$ is about 32ns, equal to about $46T_c$, which has been shown be able to capture most of the channel energy for CM1 [17]. Before we present any simulation results on BER, we first demonstrate how our proposed system provides increased data rate. Recall that in Section II, the minimum frame duration is $T_f=T_d^{\rm min}+N_h^{(1)}T_c+T_{\rm mds}$ to avoid any ISI. In the conventional TR system, $T_d^{\rm min}$ is at least equal to $T_{\rm mds}=32$ ns, while in our proposed BTR system, $T_d^{\rm min}$ can be as low as equal to $T_c=0.7$ ns. If we consider a multiuser system with $N_h^{(1)}=40$, i.e., $N_h^{(1)}T_c=28$ ns, to support at least 40 users, the minimum required T_f has been shortened from 92 ns in the conventional TR to 61 ns in the BTR system. If $N_s=4$ has been used, the data rate is increased from approximately 2.7 Mbps to 4.1 Mbps. Moreover, if $M=2$-ary orthogonal modulation is used as in the MBTR system, the data rate is further increased to 8.2 Mbps. This example clearly show the benefit of our proposed BTR and MBTR systems.

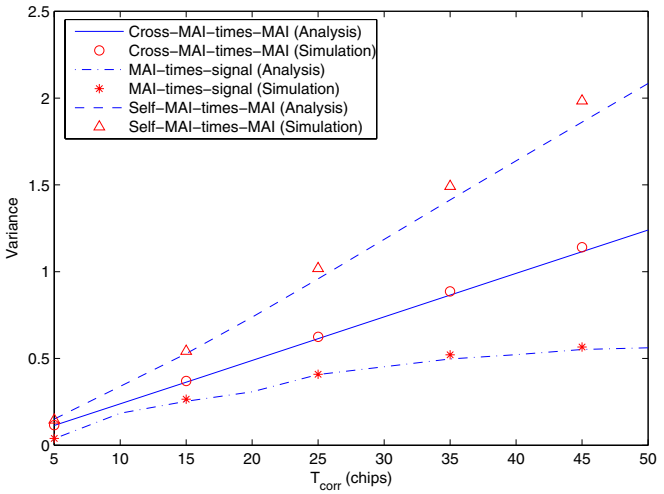

Fig. 2. Variances of I_1, I_{3B} and I_{3A} in BTR system, when $N_s=4$, $N_u=8$, $T_d^{\rm min}=10T_c$ and $N_h^{(1)}=10$.

Fig. 2 provides a validation of the analyses in Section III regarding the MAI for BTR system. Since those terms related to noise are easy to evaluate, we only present the results of the three more complicated terms I_1, I_{3B} and I_{3A}. Specifically, for one particular channel realization of CM1, we plot the three second-order moments versus different integration intervals $T_{\rm corr}$, when $N_s=4$, $N_u=8$, $T_d^{\rm min}=10T_c$, $N_h^{(1)}=10$ and the SNR per pulse is $E_p/N_o=10$ dB. Both simuation and analytical results are given. It can be seen that, for I_1 and I_{3B}, the analyses well match with the simulation results; while for I_{3A}, (27) provides a good approximation. This result also coincides with our intuition that as the integration interval $T_{\rm corr}$ increases, more MAI is introduced. Another phenomenon we can observe is self-MAI-times-MAI (dash line) is larger than cross-MAI-times-MAI (solid line) in this particular simulation. In fact, this has been stated in [12] that when the number of users is small (e.g., $N_u=8$ here), self-MAI-times-MAI dominates in the MAI-times-MAI term; while the opposite is true when the number of users is large.

In the next two figures, we provide some necessary verifications regarding the two results in Appendix B.4 and B.5,

[2]When N_s is even, the sequence is said to be balanced if the number of +1's is equal to the number of -1's, resluting in zero mean.

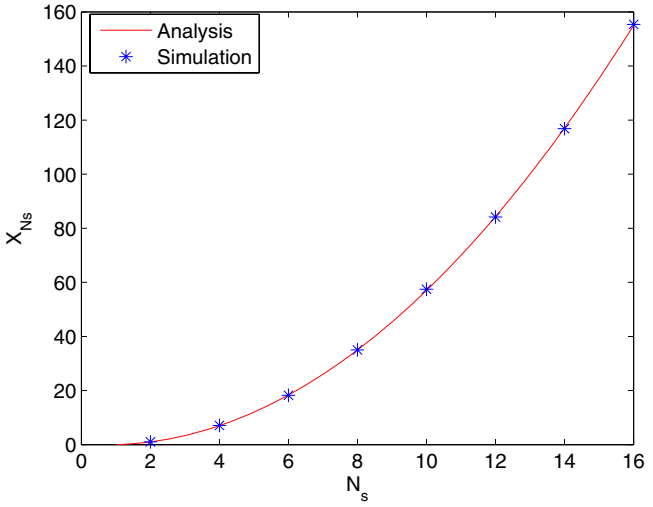

Fig. 3. Verification of (44) for different values of N_s.

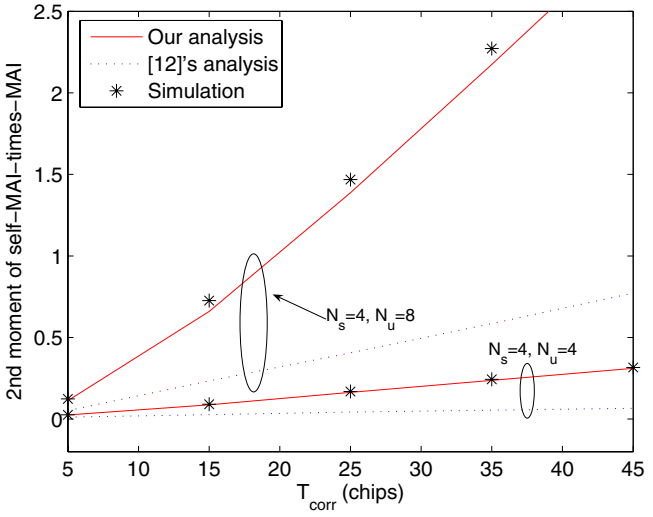

Fig. 4. Comparison of anlytical and simulation results of the second-order moment of self-MAI-times-MAI in CTR system.

respectively. In Fig. 3, we provide a validation of (44). As can be seen, the analysis well matches with the simulation results. In Fig. 4, we compare our analytical result (29) in a CTR system with the one obtained in [12], along with simulation results. Specifically, for one particular channel realization, we evaluate $\mathbf{E}\{I_{3A}^{\text{conv}2}\}$ with different integration intervals of T_{corr}, under two different scenarios. As we can see, our analysis provides more accurate match to the simulation results. The small difference between our analysis and simulation is attributed to the approximation we made in (53).

Fig. 5 numerically examines the MA performance of the BTR system averaged over 100 CM1 channel realizations, with $T_d^{\min} = 5T_c$ and $40T_c$, for $N_s = 2$ and 8, respectively. Note that $N_h^{(1)}$ is fixed to be 40, so the case of $T_d^{\min} = 5T_c$ provides higher information rate because it requires a shorter frame duration. Also, note that the maximum number of users is 32, which implies $N_h^{(32)} = 9$ according to (2). As can be seen, although the BTR system offers increased information rate by allowing a smaller $T_d^{\min}$, its BER performance in the

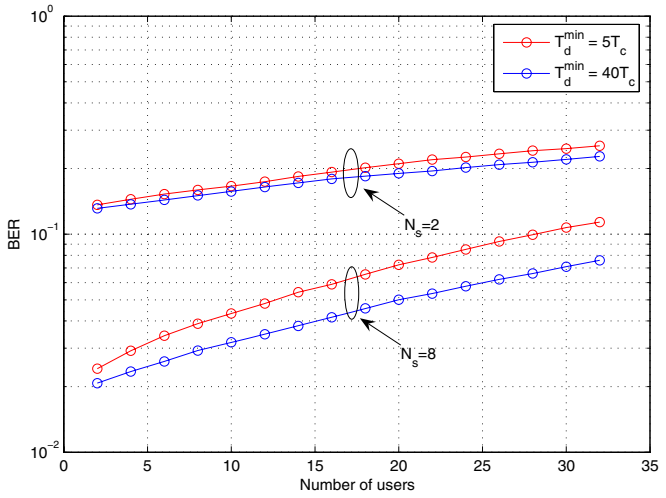

Fig. 5. BER performances for BTR system, with a fixed TH distance of $N_h^{(1)} = 40$ and $N_h^{(32)} = 9$, when $E_p/N_o = 10$ dB.

presence of MAI becomes worse, as compared to a larger $T_d^{\min}$. This is mainly because the interfering signals lying in the overlapped portion between the reference and data waveforms may incur the worst-case BER performance. As N_s increases from 2 to 8, this performance gap becomes larger because more MAI has been included. The performance results presented here also suggest that we can trade the system achievable information rate with its MA capacity. Specifically, when the number of users is small, we may allow a smaller inter-pulse distance to increase the information rate, while maintaining an acceptable BER performance. If the number of users increases, we may have to increase the inter-pulse distance to meet the BER requirement at the expense of decreased information rate.

From Fig. 5, we can see that BTR signaling does not perform well enough in a dense multiuser scenario as it does in a single user scenario [11]. To mitigate these performance degradations, we adopt M-ary orthogonal modulation on top of our BTR signaling. We foresee that, subject to the same information rate, MBTR is capable of suppressing other users' MAI, since it effectively increases the data rate, thus allows a longer frame duration, i.e., more space for TH. In Fig. 6, we compare the BER performances of $M = 2$-ary BTR with those of CTR system, under the same data rate, for $N_s = 4$ with respect to different values of $T_d^{\min}$, when $E_p/N_o = 10$ dB and 15 dB, respectively. It is obvious that, MBTR outperforms CTR for different inter-pulse distances. For instance, when $E_p/N_o = 15$ dB and subject to the BER of 10^{-2}, for all three inter-pulse distances, MBTR can support approximately 7 more users. It is also worth noting that when E_p/N_o increases from 10 to 15 dB, the performance improvement offered by a larger inter-pulse distance increases, for both MBTR and CTR systems. This is in accordance with our intuition since the higher SNR, the larger IPI can be introduced, thus separating the reference and data pulses at a larger distance are more beneficial. On the other hand, this also suggests that if the system's input SNR is low (< 10 dB), there is no need to separate the reference and data pulses at a large distance, e.g., equal to the channel delay spread, since as far as multiuser

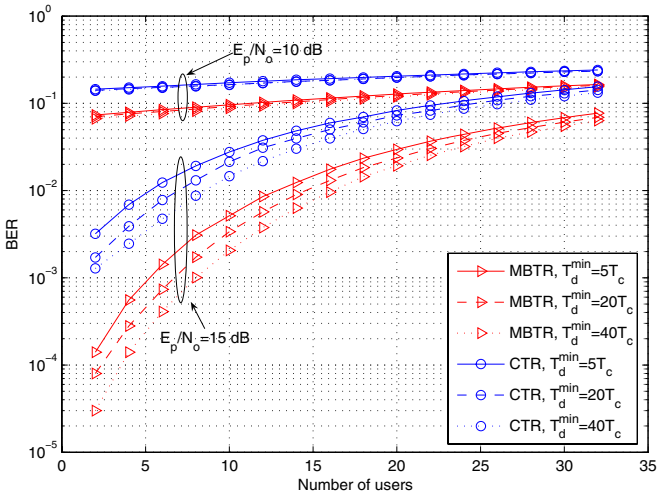

Fig. 6. BER comparison between CTR and $M = 2$-ary BTR system, subject to the same data rate, when $N_s = 4$ and $E_p/N_o = 10$ and 15 dB, respectively.

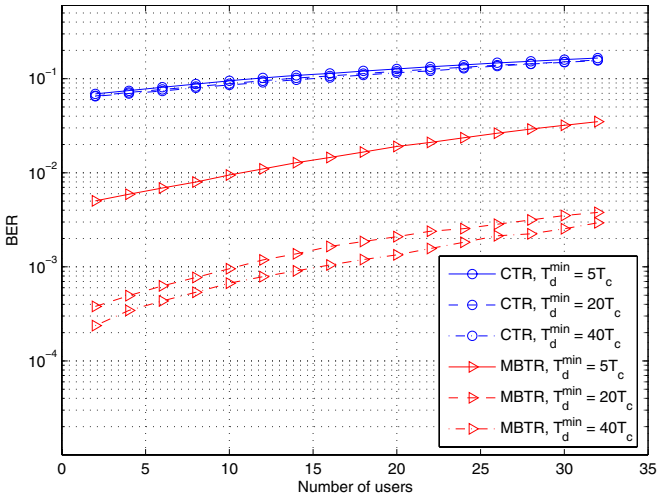

Fig. 7. BER comparison between CTR and $M = 4$-ary BTR system, subject to the same data rate, when $N_s = 8$ and $E_p/N_o = 10$ dB.

scenario is concerned, that does not improve the performance much.

In Figs. 7 and 8, we present similar performance comparisons between MBTR and CTR, while using $M = 4$-ary and $N_s = 8$ for $E_p/N_o = 10$ dB and 15 dB, respectively. Again, the same data rate is maintained for the two systems. We observe that MBTR outperforms CTR at all three inter-pulse distances. It is interesting to note that, as N_s increases from 4 to 8, the performance improvement brought by using a larger $T_d^{\min}$ becomes more significant for MBTR system, which can be observed by the larger performance gap between $T_d^{\min} = 5T_c$ and $20T_c$ or $40T_c$. In terms of the number of users, if the target BER of 10^{-3} is to be maintained under $E_p/N_o = 15$ dB in Fig. 8, MBTR can support 7, 16 and 17 more users than CTR system, for $T_d^{\min} = 5T_c$, $20T_c$ and $40T_c$, respectively. This is due to the fact that the IPI increases as N_s increases. Also, as N_s increases, the benefit from increased TH shift in MBTR system is also increasing. These two aspects suggest that when the number of frames is large, it is more

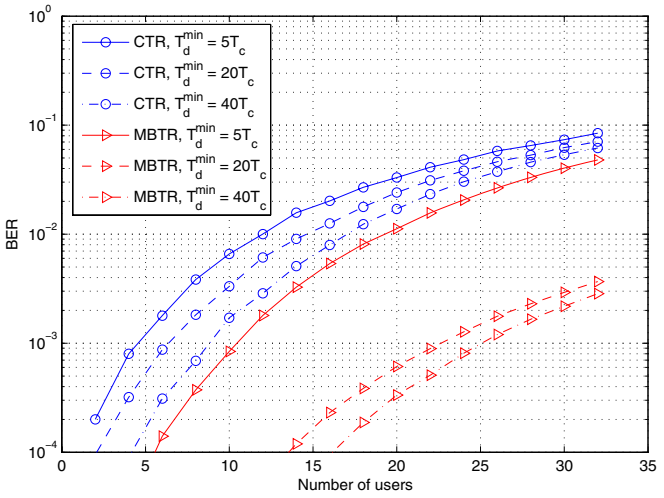

Fig. 8. BER comparison between CTR and $M = 4$-ary BTR system, subject to the same data rate, when $N_s = 8$ and $E_p/N_o = 15$ dB.

benificial to use relatively large inter-pulse distance, especially for MBTR system.

VI. Conclusion

In this paper, we evaluated the multiple access performance of balanced TR system that helps to increase the information rate with relatively low receiver complexity. We investigated its BER performance in the presence of MAI by deriving the second-order moments of all the noise and interference terms. The analyses have been verifed by simulations. It has also been demonstrated that, for the balanced TR system, a smaller inter-pulse distance may be preferred for increased information rate under limited MAI, but result in worse BER performance in dense multiuser scenario. It was also shown that the proposed balanced TR system in conjuction with M-ary orthogonal modulation offers higher MA capacity than conventional TR system, subject to the same information rate.

Appendix A

By substituting (3) into (11) and changing variables, $N_{1,j}$ can be rewritten as

$$N_{1,j} = \int_{T_d^{(1)}}^{T_d^{(1)}+T_{\text{corr}}} \left[Q_j(t)\,\tilde{n}(t-T_d^{(1)}) + Q_j(t-T_d^{(1)})\,\tilde{n}(t) \right] dt \tag{32}$$

where

$$Q_j(t) = d_j^{(1)} \left[\tilde{g}^{(1)}(t) + (-1)^j\, b_{\lfloor j/N_s \rfloor}^{(1)}\, \tilde{g}^{(1)}(t - T_d^{(1)}) \right]. \tag{33}$$

Because $N_{1,j}$ is obviously zero mean, and $N_{1,j}$ and $N_{1,j'}$ are uncorrelated for $j \neq j'$, we will have $\mathbf{E}\{{N_1}^2\} = N_s\,\mathbf{E}\{{N_{1,j}}^2\}$. Now, using (32), we can obtain

$$\mathbf{E}\{{N_{1,j}}^2\} = \mathbf{E}\left\{ \left[\int_{T_d^{(1)}}^{T_d^{(1)}+T_{\text{corr}}} Q_j(t)\,\tilde{n}(t-T_d^{(1)})\,dt \right]^2 \right\}$$

$$+\mathbf{E}\left\{\left[\int_{T_d^{(1)}}^{T_d^{(1)}+T_{\text{corr}}} Q_j(t-T_d^{(1)})\,\tilde{n}(t)\,dt\right]^2\right\}$$
$$+2\mathbf{E}\left\{\left[\int_{T_d^{(1)}}^{T_d^{(1)}+T_{\text{corr}}}\int_{T_d^{(1)}}^{T_d^{(1)}+T_{\text{corr}}} Q_j(t)\right.\right.$$
$$\left.\left.\times\,\tilde{n}(t-T_d^{(1)})Q_j(\tau-T_d^{(1)})\,\tilde{n}(\tau)\,dt\,d\tau\right]\right\}$$
$$\approx\frac{N_o}{2}\int_{T_d^{(1)}}^{T_d^{(1)}+T_{\text{corr}}}\mathbf{E}\Big\{\,Q_j^2(t)+Q_j^2(t-T_d^{(1)})\,\Big\}\,dt$$
$$+N_o\int_{T_d^{(1)}}^{T_{\text{corr}}}\mathbf{E}\Big\{\,Q_j(t+T_d^{(1)})Q_j(t-T_d^{(1)})\,\Big\}\,dt \quad (34)$$

where the approximation has been made by adopting white noise approximation for $\tilde{n}(t)$ [7]. By substituting (33) into (34), we can derive (13).

To evaluate the second-order moment of N_2, we again use the white noise approximation as done in [7], then (14) can easily be obtained.

APPENDIX B

B.1: Evaluation of $\mathbf{E}\{{I_1}^2\}$ *and* $\mathbf{E}\{{I_2}^2\}$

By substituting (3) into (15) and changing variables, $I_{1,j}$ can be rewritten as

$$I_{1,j}=\int_{T_d^{(1)}}^{T_d^{(1)}+T_{\text{corr}}}\Big[\,Q_j(t)\,\tilde{i}(t+jT_f+c_j^{(1)}T_c-T_d^{(1)})$$
$$+\,Q_j(t-T_d^{(1)})\,\tilde{i}(t+jT_f+c_j^{(1)}T_c)\Big]\,dt. \quad (35)$$

Again, $I_{1,j}$ is zero mean, $I_{1,j}$ and $I_{1,j'}$ are uncorrelated for $j\neq j'$ because of the polarity codes. Therefore, we also have $\mathbf{E}\{{I_1}^2\}=N_s\,\mathbf{E}\{{I_{1,j}}^2\}$.

Recall our assumption regarding the time asynchronous transmission delay, namely $\tau^{(\nu)}$ mod T_f is uniformly distributed over $[0,T_f)$. In other words, we assume $\tau^{(\nu)}=j^{(\nu)}T_f+\alpha^{(\nu)}$, where $j^{(\nu)}$ is an integer and $\alpha^{(\nu)}$ is uniformly distributed over $[0,T_f)$. Based on this assumption, we can easily find that, there will be only two frames' signal from each interferer affecting the desired user's jth frame's reception, which are the $[j-j^{(\nu)}]$th and $[j-j^{(\nu)}-1]$th frames, hereafter referred to as the *current* and the *previous* frames, respectively.

We divide the integrations over the two integrands in (35) into two parts, denoted by $I_{1,j,a}$ and $I_{1,j,b}$, respectively. This will lead to

$$\mathbf{E}\{{I_{1,j}}^2\}=\mathbf{E}\{{I_{1,j,a}}^2\}+\mathbf{E}\{{I_{1,j,b}}^2\}+2\mathbf{E}\{I_{1,j,a}I_{1,j,b}\}. \quad (36)$$

First, by substituting the current and the previous frames' interfering signal, we have

$$I_{1,j,a}=\sum_{\nu=2}^{N_u}\int_{T_d^{(1)}}^{T_d^{(1)}+T_{\text{corr}}}Q_j(t)\Big\{d_{j-j^{(\nu)}}^{(\nu)}\Big[\tilde{g}^{(\nu)}(t-\theta_{j,j^{(\nu)}}-T_d^{(1)})$$
$$+(-1)^{j-j^{(\nu)}}\,b^{(\nu)}_{\lfloor\frac{j-j^{(\nu)}}{N_s}\rfloor}\,\tilde{g}^{(\nu)}(t-\theta_{j,j^{(\nu)}}-T_d^{(1)}-T_d^{(\nu)})\Big]$$
$$+\,d_{j-j^{(\nu)}-1}^{(\nu)}\Big[\tilde{g}^{(\nu)}(t-\theta_{j,j^{(\nu)}+1}+T_f-T_d^{(1)})+(-1)^{j-j^{(\nu)}-1}$$
$$\times\,b^{(\nu)}_{\lfloor\frac{j-j^{(\nu)}-1}{N_s}\rfloor}\tilde{g}^{(\nu)}(t-\theta_{j,j^{(\nu)}+1}-T_d^{(1)}+T_f-T_d^{(\nu)})\Big]\Big\}\,dt \quad (37)$$

where $\theta_{j,\,j^{(\nu)}}\triangleq[c_{j-j^{(\nu)}}^{(\nu)}-c_j^{(1)}]T_c+\alpha^{(\nu)}$. Furthermore, we can divide $I_{1,j,a}$ into two parts, according to the two components of $Q_j(t)$. It is easy to verify that those two parts of $I_{1,j,a}$ are uncorrelated to each other, because the data bit $b^{(1)}_{\lfloor j/N_s\rfloor}$ takes on ±1 with equal probabilities. Therefore, we can evaluate the second-order moments of the two separately. Then, by taking the average over all users' possible TH codes and $\alpha^{(\nu)}$ for $\nu=2,3,\ldots,N_u$, as well as considering the support range of (17), we can easily obtain

$$\mathbf{E}\{{I_{1,j,a}}^2\}=\frac{2}{T_f}\sum_{\nu=2}^{N_u}\int_{-\infty}^{+\infty}\Big[\,R_{1\nu}^2(\tau,T_d^{(1)})+R_{1\nu}^2(\tau,0)\,\Big]\,d\tau. \quad (38)$$

Similarly, we can obtain

$$\mathbf{E}\{{I_{1,j,b}}^2\}=\frac{2}{T_f}\sum_{\nu=2}^{N_u}\int_{-\infty}^{+\infty}\Big[R_{1\nu}^2(\tau,0)+R_{1\nu}^2(\tau-T_d^{(1)},-T_d^{(1)})\Big]\,d\tau \quad (39)$$

$$\mathbf{E}\{I_{1,j,a}I_{1,j,b}\}=\frac{2}{T_f}\sum_{\nu=2}^{N_u}\int_{-\infty}^{+\infty}\Big[R_{1\nu}(\tau+T_d^{(1)},T_d^{(1)})$$
$$\times\,R_{1\nu}(\tau-T_d^{(1)},0)R_{1\nu}(\tau,0)R_{1\nu}(\tau-T_d^{(1)},-T_d^{(1)})\Big]d\tau. \quad (40)$$

By combining (36), (38), (39) and (40), we can finally obtain (16).

The evaluation of $\mathbf{E}\{{I_2}^2\}$ is similar to $\mathbf{E}\{{N_1}^2\}$. We omit the detailed derivation for simplicity.

B.2: Proof of Lemma 1

We can express $I_{3A,j}$ as $I_{3A,j}\triangleq\sum_{\nu=2}^{N_u}I_{3A,j}^{(\nu)}$, where

$$I_{3A,j}^{(\nu)}=R_{\nu\nu}(-T_d^{(1)},-\theta_{j,j^{(\nu)}}^{(\nu)})+(-1)^{j-j^{(\nu)}}b^{(\nu)}_{\lfloor\frac{j-j^{(\nu)}}{N_s}\rfloor}$$
$$\times\,R_{\nu\nu}(-T_d^{(1)}-T_d^{(\nu)},-\theta_{j,j^{(\nu)}}^{(\nu)}-T_d^{(\nu)})$$
$$+(-1)^{j-j^{(\nu)}}b^{(\nu)}_{\lfloor\frac{j-j^{(\nu)}}{N_s}\rfloor}\,R_{\nu\nu}(-T_d^{(1)}+T_d^{(\nu)},-\theta_{j,j^{(\nu)}}^{(\nu)})$$
$$+\,R_{\nu\nu}(-T_d^{(1)},-\theta_{j,j^{(\nu)}}^{(\nu)}-T_d^{(\nu)})+d_{j-j^{(\nu)}}^{(\nu)}d_{j-j^{(\nu)}-1}^{(\nu)}$$
$$\times\,(-1)^{j-j^{(\nu)}-1}b^{(\nu)}_{\lfloor\frac{j-j^{(\nu)}-1}{N_s}\rfloor}R_{\nu\nu}(T_f-T_d^{(1)}-$$
$$-\,T_d^{(\nu)}+\theta_{j,j^{(\nu)}}^{(\nu)}-\theta_{j,j^{(\nu)}+1}^{(\nu)},T_f-\theta_{j,j^{(\nu)}+1}^{(\nu)}-T_d^{(\nu)})$$
$$+\,R_{\nu\nu}(-T_d^{(1)},T_f-\theta_{j,j^{(\nu)}+1}^{(\nu)})+(-1)^{j-j^{(\nu)}-1}\,b^{(\nu)}_{\lfloor\frac{j-j^{(\nu)}-1}{N_s}\rfloor}$$
$$\times\,R_{\nu\nu}(-T_d^{(1)}-T_d^{(\nu)},T_f-\theta_{j,j^{(\nu)}+1}^{(\nu)}-T_d^{(\nu)})$$
$$+\,(-1)^{j-j^{(\nu)}-1}b^{(\nu)}_{\lfloor\frac{j-j^{(\nu)}-1}{N_s}\rfloor}R_{\nu\nu}(T_d^{(1)}-T_d^{(\nu)},T_f-\theta_{j,j^{(\nu)}+1}^{(\nu)})$$
$$+\,R_{\nu\nu}(-T_d^{(1)},T_f-\theta_{j,j^{(\nu)}+1}^{(\nu)}-T_d^{(\nu)}). \quad (41)$$

Though very complicated, the nine terms in (41) have represented all possible collision events in characterizing the self-MAI-times-MAI term. When taking the expectation for (41), we can easily find that only the 1st, 4th, 6th and 9th terms are non-zero and all others become zero due to the random polarity codes as well as data bits. Furthermore, the sum of the 1st, 4th, 6th and 9th terms, after taking the expectation, will no longer depend on the frame index j, leading to

$$\mathbf{E}\{I_{3A,j}\}=\frac{2T_{\text{corr}}}{T_f}\sum_{\nu=2}^{N_u}\int_{-\infty}^{+\infty}\tilde{g}^{(\nu)}(x+T_d^{(1)})\,\tilde{g}^{(\nu)}(x)\,dx. \quad (42)$$

Based on (42), we will have

$$\mathbf{E}\{I_{3A}\} = \sum_{j}(-1)^j \mathbf{E}\{I_{3A,j}\} = \mathbf{E}\{I_{3A,j}\} \sum_{j=iN_s}^{(i+1)N_s-1} (-1)^j = 0.$$

Note that this zero-mean property stems from the *balanced* TR signaling.

B.3: Evaluation of $\mathbf{E}\{{I_{3B}}^2\}$

Rather than nine terms in $I_{3A,j}$ given by (41), the expression of $I_{3B,j}$ includes sixteen terms, which again have included all possible collision events in characterizing the cross-MAI-times-MAI term. Fortunately, it is easy to verify that, due to the usage of the user-specific random polarity codes and data bits, those sixteen terms are *uncorrelated* to each other. Bearing this in mind, the second-order moment of $I_{3B,j}$ can simply be written as the sum of the second-order moments of those sixteen terms, finally leading to (26).

B.4: Evaluation of $\mathbf{E}\{{I_{3A}}^2\}$

The evaluation of $\mathbf{E}\{{I_{3A}}^2\}$ is much more complicated as compared to $\mathbf{E}\{{I_{3B}}^2\}$, since the nine terms in (41) have some correlations, yielding an exact result less tractable. Therefore, we make some necessary simplifications and will validate it in the results section.

First of all, we have

$$\mathbf{E}\{I_{3A}^2\} = \sum_{\nu=2}^{N_u}\Bigg[\sum_{j}\mathbf{E}\{{I_{3A,j}^{(\nu)}}^2\} + \sum_{j}\sum_{j'\neq j}(-1)^j(-1)^{j'}\,\mathbf{E}\{I_{3A,j}^{(\nu)}\,I_{3A,j'}^{(\nu)}\}\Bigg]. \quad (43)$$

When evaluating the first term in (43), i.e., $\mathbf{E}\{I_{3A,j}^2\}$, we ignore the cross-terms among all nine terms in (41) and only count their second-order moments. This gives the first and second integrations in (27). When evaluating the second term in (43), i.e., $\mathbf{E}\{I_{3A,j}I_{3A,j'}\}$, we adopt a similar simplification method and utilize the following equation

$$X_{N_s} \triangleq \sum_{j}\sum_{j'\neq j}\mathbf{E}\Big[b^{(\nu)}_{\lfloor\frac{j-j^{(\nu)}}{N_s}\rfloor}\,b^{(\nu)}_{\lfloor\frac{j'-j^{(\nu)}}{N_s}\rfloor}\Big] = \frac{1}{3}(N_s-1)(2N_s-1). \quad (44)$$

Note that X_{N_s} represents the correlation among the data bits indexed by j and j', considering $j^{(\nu)}$ as a random variable. The proof of (44) is left to readers and it will be verified in the results section. Finally, we can derive the rest of (27).

B.5: Evaluation of $\mathbf{E}\{I_{3A}^{conv2}\}$

As a special case, in CTR system where $T_d^{\min} \geq T_{\text{mds}}$, only the 3rd, 5th and 8th terms in (41) are left and all others become zero, rewritten as

$$\begin{aligned} I_{3A,j}^{\text{conv}} = \sum_{\nu=2}^{N_u}\Bigg[& b^{(\nu)}_{\lfloor\frac{j-j^{(\nu)}}{N_s}\rfloor}\,R_{\nu\nu}(-T_d^{(1)}+T_d^{(\nu)}, -\theta^{(\nu)}_{j,j^{(\nu)}}) \\ & + b^{(\nu)}_{\lfloor\frac{j-j^{(\nu)}-1}{N_s}\rfloor}\,R_{\nu\nu}(T_d^{(1)}-T_d^{(\nu)}, T_f-\theta^{(\nu)}_{j,j^{(\nu)}+1}) \\ & + d^{(\nu)}_{j-j^{(\nu)}}\,d^{(\nu)}_{j-j^{(\nu)}-1}\,b^{(\nu)}_{\lfloor\frac{j-j^{(\nu)}-1}{N_s}\rfloor}\,R_{\nu\nu}(T_f-T_d^{(1)} \\ & - T_d^{(\nu)}+\theta^{(\nu)}_{j,j^{(\nu)}}-\theta^{(\nu)}_{j,j^{(\nu)}+1}, T_f-\theta^{(\nu)}_{j,j^{(\nu)}+1}-T_d^{(\nu)})\Bigg]. \end{aligned} \quad (45)$$

Note that there is no $(-1)^j$ weighting factor in CTR system. For notationaly simplicity, we denote the three terms in (45) as $\Phi_j^{(\nu)}$, $\Psi_j^{(\nu)}$ and $\Gamma_j^{(\nu)}$, respectively. Then, the total self-MAI-times-MAI term I_{3A}^{conv} can be written as

$$I_{3A}^{\text{conv}} = \sum_{j=iN_s}^{(i+1)N_s-1} I_{3A,j}^{\text{conv}} = \sum_{\nu=2}^{N_u}\sum_{j=iN_s}^{(i+1)N_s-1}\Big[\Phi_j^{(\nu)}+\Psi_j^{(\nu)}+\Gamma_j^{(\nu)}\Big]. \quad (46)$$

Thus, we have

$$\begin{aligned} \mathbf{E}\{I_{3A}^{\text{conv}2}\} = \sum_{\nu=2}^{N_u}\sum_{\nu'=2}^{N_u}\sum_{j=iN_s}^{(i+1)N_s-1}\sum_{j'=iN_s}^{(i+1)N_s-1}\mathbf{E}\Bigg\{\Big[\Phi_j^{(\nu)}+\Psi_j^{(\nu)} \\ +\Gamma_j^{(\nu)}\Big]\times\Big[\Phi_{j'}^{(\nu')}+\Psi_{j'}^{(\nu')}+\Gamma_{j'}^{(\nu')}\Big]\Bigg\}. \end{aligned} \quad (47)$$

It is straightforward to see that if $\nu \neq \nu'$, the expectation goes to zero due to random polarity codes and data bits, yielding

$$\begin{aligned} \mathbf{E}\{I_{3A}^{\text{conv}2}\} = \sum_{\nu=2}^{N_u}\sum_{j}\sum_{j'}\mathbf{E}\Bigg\{\Big[\Phi_j^{(\nu)}+\Psi_j^{(\nu)}+\Gamma_j^{(\nu)}\Big] \\ \times\Big[\Phi_{j'}^{(\nu)}+\Psi_{j'}^{(\nu)}+\Gamma_{j'}^{(\nu)}\Big]\Bigg\}. \end{aligned} \quad (48)$$

Here, we have omitted the summation limits of j and j' for notational simplicity. Now, depending on whether $j=j'$ or not, we separate (48) into two uncorrelated terms as V_{I} and V_{II}, respectively.

$$\begin{aligned} V_{\text{I}} &= \sum_{\nu=2}^{N_u}\sum_{j}\mathbf{E}\Bigg\{\Big[\Phi_j^{(\nu)}+\Psi_j^{(\nu)}+\Gamma_j^{(\nu)}\Big]^2\Bigg\} \\ &= \sum_{\nu=2}^{N_u}\sum_{j}\mathbf{E}\Big[{\Phi_j^{(\nu)}}^2+{\Psi_j^{(\nu)}}^2+{\Gamma_j^{(\nu)}}^2\Big] \end{aligned} \quad (49)$$

where the expectations of the cross-terms in (49) become zero again because of the polarity codes and data bits. Finally, we have

$$\mathbf{E}\Big[{\Phi_j^{(\nu)}}^2+{\Psi_j^{(\nu)}}^2\Big] = \frac{1}{T_f}\int_{-T_{\text{corr}}}^{T_{\text{mds}}} R_{\nu\nu}^2(T_d^{(\nu)}-T_d^{(1)},x)\,dx \quad (50)$$

$$\begin{aligned} \mathbf{E}\Big[{\Gamma_j^{(\nu)}}^2\Big] = \frac{1}{T_f}\sum_{h\in\mathcal{H}^{(\nu)}}\frac{N_h^{(\nu)}-|h|}{{N_h^{(\nu)}}^2} \\ \times\int_{-T_{\text{corr}}}^{T_{\text{mds}}} R_{\nu\nu}^2(T_f-T_d^{(1)}-T_d^{(\nu)}-hT_c,x)dx. \end{aligned} \quad (51)$$

On the other hand,

$$\begin{aligned} V_{\text{II}} &= \sum_{\nu=2}^{N_u}\sum_{j}\sum_{j'\neq j}\mathbf{E}\Big\{\Big[\Phi_j^{(\nu)}+\Psi_j^{(\nu)}+\Gamma_j^{(\nu)}\Big]\Big[\Phi_{j'}^{(\nu)}+\Psi_{j'}^{(\nu)}+\Gamma_{j'}^{(\nu)}\Big]\Big\} \\ &= \sum_{\nu=2}^{N_u}\sum_{j}\sum_{j'\neq j}\mathbf{E}\Big[\Phi_j^{(\nu)}\Phi_{j'}^{(\nu)}+\Phi_j^{(\nu)}\Psi_{j'}^{(\nu)}+\Psi_j^{(\nu)}\Phi_{j'}^{(\nu)}+\Psi_j^{(\nu)}\Psi_{j'}^{(\nu)}\Big] \end{aligned} \quad (52)$$

where those five terms that have vanished from (52) are again due to the polarity codes and data bits. In our simulations, we find that

$$\mathbf{E}\Big[\Phi_j^{(\nu)}\Psi_{j'}^{(\nu)}+\Psi_j^{(\nu)}\Phi_{j'}^{(\nu)}\Big] \ll \mathbf{E}\Big[\Phi_j^{(\nu)}\Phi_{j'}^{(\nu)}+\Psi_j^{(\nu)}\Psi_{j'}^{(\nu)}\Big], \quad (53)$$

which is thus ignored in the final expression as

$$\mathbf{E}\left[\Phi_j^{(\nu)}\Phi_{j'}^{(\nu)} + \Psi_j^{(\nu)}\Psi_{j'}^{(\nu)}\right] = \frac{(N_s-1)(2N_s-1)}{3N_s T_f} \times \sum_{h_1\in\mathcal{H}^{(\nu)}} \sum_{h_2\in\mathcal{H}^{(1)}} \frac{N_h^{(\nu)} - |h_1|}{{N_h^{(\nu)}}^2} \times \frac{N_h^{(1)} - |h_2|}{{N_h^{(1)}}^2} \times \int_{-T_{\text{corr}}}^{T_{\text{mds}}} R_{\nu\nu}(T_d^{(\nu)} - T_d^{(1)}, x) \times R_{\nu\nu}(T_d^{(\nu)} - T_d^{(1)}, x + h_1 T_c + h_2 T_c)\, dx. \quad (54)$$

Note that, in deriving (54), we have used (44). Finally, by substituting (54) into (52), (50) and (51) into (49), then into (48), we can obtain (29). In the results section, we will compare (29) with the corresponding (2nd last) term of eq. (21) in [12], along with simulation results.

REFERENCES

[1] C. Rushforth, "Transmitted-reference techniques for random or unknown channels," *IEEE Trans. Inform. Theory*, vol. 10, pp. 39-42, Jan 1964.

[2] R. Gagliardi, "A geometrical study of transmitted reference communication system," *IEEE Commun. Lett.*, pp. 118-123, Dec. 1964.

[3] R. Hoctor and H. Tomlinson, "Delay-hopped transmitted-reference RF communications," in *IEEE Proc. UWBST*, May 2002, pp. 265-269.

[4] J. D. Choi and W. E. Stark, "Performance of ultra-wideband communications with suboptimal receivers in multipath channels," *IEEE J. Select. Areas Commun.*, vol. 20, pp. 1754-1766, Dec. 2002.

[5] Y. Chao and R. A. Scholtz, "Optimal and suboptimal receivers for ultra-wideband transmitted reference systems," in *IEEE Proc. Global Telecommun.*, Dec. 2003, vol. 2, pp. 759-763.

[6] Y. Chao and R. A. Scholtz, "Ultra-wideband transmitted reference systems," *IEEE Trans. Veh. Technol.*, vol. 54, pp. 1556-1568, Sep. 2005.

[7] T. Q. S. Quek and M. Z. Win, "Analysis of UWB transmitted-reference communication systems in dense multipath channels," *IEEE J. Select. Areas Commun.*, vol. 23, no. 9, pp. 1863-1874, Sep. 2005.

[8] K. Witrisal, G. Leus, M. Pausini, and C. Krall, "Equivalent system model and equalization of differential impulse radio UWB systems," *IEEE J. Select. Areas Commun.*, vol. 23, no. 9, pp. 1851-1862, Sep. 2005.

[9] K. Witrisal and M. Pausini, "Statistical analysis of transmitted-reference UWB systems on multipath channels," in *IEEE Proc. ICUWB*, Sep. 2006, pp. 303-308.

[10] Z. Xu, B. M. Sadler, and J. Tang "Data detection for UWB transmitted reference systems with inter-pulse interfrence" *IEEE Proc. ICASSP*, vol. 3, pp. 601-604, Mar. 2005.

[11] D. I. Kim and T. Jia, "M-ary orthogonal coded/balanced UWB transmitted-reference system," in *Proc. IEEE ICC*, June 2006, vol. 12, pp. 5552-5557.

[12] Y. Chao and R. A. Scholtz, "Multiple access performance of ultra-wideband transmitted reference systems in multipath environments," in *Proc. IEEE WCNC*, Mar. 2004, vol. 3, pp. 1788-1793.

[13] Z. Xu and B. M. Sadler, "Multiuser transmitted reference ultra-wideband communication systems" *IEEE J. Select. Areas Commun.*, vol. 24, no. 4, pp. 766-772, Apr. 2006.

[14] S. Gezici, Z. Sahinoglu, H. Kobayashi, and H. V. Poor, "Ultra-wideband impulse radio systems with multiple pulse types" *IEEE J. Select. Areas Commun.*, vol. 24, no. 4, pp. 892-898, Apr. 2006.

[15] X. Dong, A. C. Y. Lee, and L. Xiao, "A new UWB dual pulse transmission and detection technique," *Proc. IEEE ICC*, May 2005, vol. 4, no. 4, pp. 2835-2839.

[16] L. Wu, X. Wu, and Z. Tian, "Asymptotically optimal UWB receivers with noisy templates: design and comparison with r ake," *IEEE J. Select. Areas Commun.*, vol. 24, pp. 808-814, Apr. 2006.

[17] T. Jia and D. I. Kim, "Analysis of channel-averaged SINR for indoor UWB rake and transmitted reference systems," *IEEE Trans. Commun.*, vol. 55, no. 10, pp. 2022-2032, Oct. 2007.

[18] A. F. Molisch, J. R. Foerster, and M. Pendergrass, "Channel models for ultrawideband personal area networks," *IEEE Pers. Commun. Mag.*, vol. 10, pp. 14-21, Dec. 2003.

Tao Jia (S'05) received the B.Eng. degree in Electrical Engineering from University of Science and Technology of China (USTC), Hefei, in 2003, and the M.A.Sc. degree in Electrical Engineering from Simon Fraser University, Burnaby, Canada, in 2006.

He is now with the Bradley Department of Electrical and Computer Engineering, Virginia Polytechnic Institute and State University (Virginia Tech), Blacksburg, VA, where he is working for a Ph.D. degree in the Mobile and Portable Radio Research Group (MPRG). His research interests include position location in wireless sensor networks, physical layer design and performance analysis for UWB communication systems, software defined radio (SDR), and cognitive radio system.

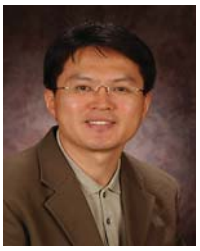

Dong In Kim (S'89-M'91-SM'02) received the B.S. and M.S. degrees in Electronics Engineering from Seoul National University, Seoul, Korea, in 1980 and 1984, respectively, and the M.S. and Ph.D. degrees in Electrical Engineering from the University of Southern California (USC), Los Angeles, in 1987 and 1990, respectively.

From 1984 to 1985, he was a Researcher with Korea Telecom Research Center, Seoul. From 1986 to 1988, he was a Korean Government Graduate Fellow in the Department of Electrical Engineering, USC. From 1991 to 2002, he was with the University of Seoul, Korea, leading the Wireless Communications Research Group. From 2002 to 2007, he was a tenured Full Professor in the School of Engineering Science, Simon Fraser University, Burnaby, BC, Canada. From 1999 to 2000, he was a Visiting Professor at the University of Victoria, Victoria, BC. Since 2007, he has been with Sungkyunkwan University (SKKU), Suwon, Korea, where he is a Professor and SKKU Fellow in the School of Information and Communication Engineering. Since 1988, he is engaged in the research activities in the areas of cellular radio networks and spread-spectrum systems. His current research interests include 4G systems, ultra-wideband (UWB) multi-gigabyte short-range transmission, cooperative communications and cognitive radios, and cross-layer design.

Dr. Kim was an Editor for the IEEE JOURNAL ON SELECTED AREAS IN COMMUNICATIONS: WIRELESS COMMUNICATIONS SERIES and also a Division Editor for the *Journal of Communications and Networks*. He is currently an Editor for Spread Spectrum Transmission and Access for the IEEE TRANSACTIONS ON COMMUNICATIONS and an Editor for the IEEE TRANSACTIONS ON WIRELESS COMMUNICATIONS. He also serves as Co-Editor-in-Chief for the *Journal of Communications and Networks*.